Laser and Particle Beams (2010), *28*, 585–590.

doi:10.1017/S0263034610000650

Enhancement of monoenergetic proton beams *via* cone substrate in high intensity laser pulse-double layer target interactions

WEIMIN ZHOU,[1] YUQIU GU,[1] WEI HONG,[1] LEIFENG CAO,[1] ZONGQING ZHAO,[1] YONGKUN DING,[1] BAOHAN ZHANG,[1] HONGBO CAI,[2] AND KUNIOKI MIMA[3]

[1]Research Center of Laser Fusion, China Academy of Engineering Physics, Mianyang, Sichuan, China
[2]Institute of Applied Physics and Computational Mathematics, Beijing, China
[3]Institute of laser Engineering, Osaka University, Suita, Osaka, Japan

(RECEIVED 21 March 2010; ACCEPTED 16 October 2010)

Abstract

A scheme capable of enhancing the energy of monoenergetic protons in high intensity laser-plasma interactions is proposed and demonstrated by two dimensional particle-in-cell simulations. The focusing of laser light pulse and the guiding of surface current *via* the high *Z* material cone-shaped substrate increase the temperature of hot electrons, which are responsible for the electrostatic field accelerating protons. Moreover, the sub-micron proton layer coated on the cone-shaped substrate makes the total proton beam experience the same accelerating field, thus the monochromaticity is maintained. Compared to the normal film double layer target, the energy of monoenergetic proton beams can be improved about three times.

Keywords: Laser-plasma interaction; Monoenergetic proton beams; PIC simulation

INTRODUCTION

One of the significant achievements of high-intensity laser plasma interaction is the generation of high energy ion beams, which is of potential applications in cancer therapy (Bulanov *et al.*, 2002), inertial confinement fusion (Roth *et al.*, 2001), diagnostics of high density matter (Borghesi *et al.*, 2002; Li *et al.*, 2008). Over the last two decades, a number of experiments on the generation of forward multi-MeV ions for chirped pulse amplification laser lights at intensities over 10^{18} W/cm^2 were reported and interpreted with remarkably different mechanisms (Clark *et al.*, 2000; Maksimchuk *et al.*, 2000; Snavely *et al.*, 2000) for origin and acceleration. The full discussion of the model proposed by Snavely *et al.* (2000) was presented and demonstrated by particle-in-cell (PIC) simulation (Wilks *et al.*, 2001), which is termed the target normal sheath acceleration (TNSA) mechanism. From Poisson's equation and Boltzmann statistics for electrons, the accelerating electric fields acting on the ions was estimated as $E = T_h/e \max(L_n, \lambda_D)$, here T_h is the temperature of hot electrons, L_n is the density scale length of plasma, and λ_D is the Debye length.

The potential applications of the laser induced ions require the energy and intensity of ions should be high enough. Mass-limited target design was shown to enhance the ion energy significantly due to the increase in the hot electron concentration (Limpouch *et al.*, 2008). Moreover, a new laser ion acceleration mechanism named laser break-out afterburner (BOA) suggested that GeV ions could be achieved from ultrathin target (Yin *et al.*, 2006). However, the currently available ultrashort laser facilities around the world can not meet the super high laser contrast requirement of the BOA mechanism. To improve the intensity of laser ions, circularly polarized laser pulse was demonstrated to collimate the ion beams (Kado *et al.*, 2006). Furthermore, a permanent magnet lens system was used to achieve both collimation and monochromatisation of the laser ions (Ter-Avetisyan *et al.*, 2008).

The typical energy spectrum of accelerated ions has a quasi-thermal distribution with a cutoff energy, namely, their spectrum has almost 100% spread. However, applications of high-energy ions require high-quality ion beams with small energy spread. In order to obtain quasi-monoenergetic proton beams, a scheme using microstructured double-layer

Address correspondence and reprint requests to: Weimin Zhou, Research Center of Laser Fusion, China Academy of Engineering Physics, Mianyang, Sichuan Province 621900, China. E-mail: zhouweimin@gmail.com

target was proposed and demonstrated by three-dimensional PIC simulations (Esirkepov *et al.*, 2002). Experiments based on the scheme in Esirkepov *et al.* (2002) was carried out successfully (Schwoerer *et al.*, 2006).

Critical for the acceleration of monoenergetic protons is the absorption efficiency of laser energy to hot electrons, since protons are accelerated by the electric fields induced by the charge separation of hot electrons and background ions. A target design of the re-entrant cone geometry (Kodama *et al.*, 2001) for fast ignition has attracted considerable interest. PIC simulations proved the cone target can increase the energy coupling from the laser pulse to electrons effectively *via* the focusing of laser light pulse (Sentoku *et al.*, 2004) and the guiding of surface current (Nakamura *et al.*, 2004). A cone target is also proposed to enhance the generation of protons in simulation (Nakamura *et al.*, 2008) and experiment (Flippo *et al.*, 2008). But in these two references, the energy spreads of accelerated protons are almost 100% and it is not clear that if the cone target will damage the monochromaticity of protons.

In this paper, a scheme to increase the energy of quasi-monoenergetic protons is proposed. In this scheme, a cone-shaped target of high-Z material is used to interact with an intense laser light for improving the generation and confinement of hot electrons. The rear surface of this target is coated with an extra sub-micron proton layer with relatively low density to act as the source of proton for the acceleration. Due to the proton acceleration mechanisms, protons are accelerated by the sheath field produced by hot electrons on the boundary between the high-Z substrate and the proton layer. As a result, the higher energy and density of hot electrons in the cone target increase the proton energy.

PIC SIMULATIONS

Two-dimensional fully relativistic electro-magnetic PIC simulations were performed to investigate the above process. Our two-dimensional PIC code is FLIPS2D, with the finite difference method to solve the field equations and Boris' method to calculate the particle motion (Birdsall & langdon, 1991). Besides, the charge conservation method of first-order weighting of particles is exploited to make the simulation run faster (Umeda *et al.*, 2003). The scales of the simulation box are $X \times Y = 60\lambda_0 \times 40\lambda_0$ with a cell size of $\Delta X = \Delta Y = 0.02\lambda_0$, where λ_0 is the wavelength of the incident laser light. A linearly polarized Gaussian laser beam with a focal spot of $6\lambda_0$ (full width at half maximum) is incident to the simulation box along the X axis from left to right. The laser beam rises up in $5\tau_0$, with a sinusoidal profile, after which it maintains its peak intensity for $20\tau_0$, and then falls to zero in another $5\tau_0$, where τ_0 is the laser period. The peak normalized vector potential is $a_0 = eA/m_e\omega_0 c^2 = 5.0$, which corresponds to the peak incident intensity $I_0 = 3.5 \times 10^{19}$ W/cm^2.

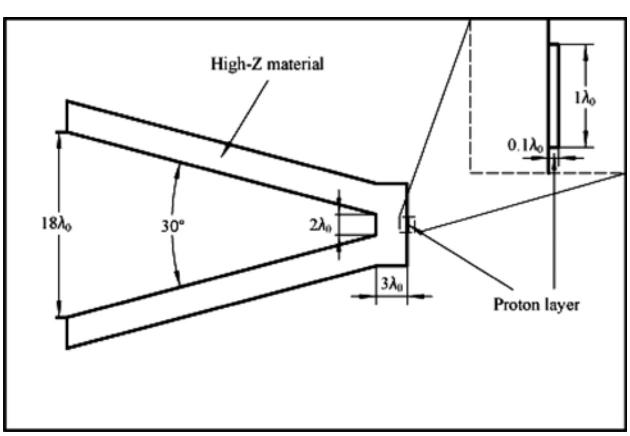

Fig. 1. Schematic of the cone-shaped substrate and the coated proton layer.

The geometry of the cone-shaped substrate and coated proton layer is shown in Figure 1. The width of the cone wall is $3\lambda_0$, the open hatch and the tip are $18\lambda_0$ and $2\lambda_0$ wide, respectively, and the open angle is 30°, which is the optimum angle for laser-cone interactions (Nakamura *et al.*, 2008). The cone substrate consists of partially ionized plasma where the effective charge-to-mass ratio Z/A is assumed to be 1/10. The electron density of the target is 10 times the critical density (n_c), which is related to the frequency of the incident laser as $\omega_0^2 = 4\pi e^2 n_c/m_e$. The initial electron and ion temperatures are both 1.0 keV. At the rear surface of the cone substrate, there is a proton layer with density of n_c.

To demonstrate the advantage of cone target for laser proton acceleration, a scheme with film substrate is simulated. For the film target, the high-Z layer is $18\lambda_0$ wide and $3\lambda_0$ thick. The proton layers for cone substrate and film are both $1\lambda_0$ wide and $0.1\lambda_0$ thick. Because the protons on the target's rear surface are accelerated directly by the sheath field due to the TNSA mechanism, first evolution of the on-axis distributions of sheath fields for cone and film targets is plotted in Figure 2. We can see that at all times the amplitude and the range of the electric field on the rear surface of the cone target (solid line) is much higher than those for the film target (dashed line), as expected. The electrostatic field's higher and wider amplitude indicates higher acceleration for the cone target.

Enhancement of the sheath field is believed to result from the increase of hot electrons generated by the cone target. From the TNSA mechanism, the amplitude of the sheath field on the target's rear surface is proportional to the temperature of hot electrons (not thermal electrons). When an intense laser light interacts with the side wall of the cone target, electrons are confined on the surface to the tip by the self-induced surface magnetic field (Nakamura *et al.*, 2004). Meanwhile, the laser pulse is focused by the conical surface (Sentoku *et al.*, 2004), and its intensity can be increased by a few of times. The temperature of hot electrons is $T_h = 511[(1 + 0.73 I_{10^{18}\mathrm{W/cm^2}} \lambda_{\mu m}^2)^{1/2} - 1]$ keV due to the $J \times B$ mechanism (Wilks *et al.*, 1992) predominant in this regime. Thus, the temperature of hot electrons is increased

https://doi.org/10.1017/S0263034610000650 Published online by Cambridge University Press

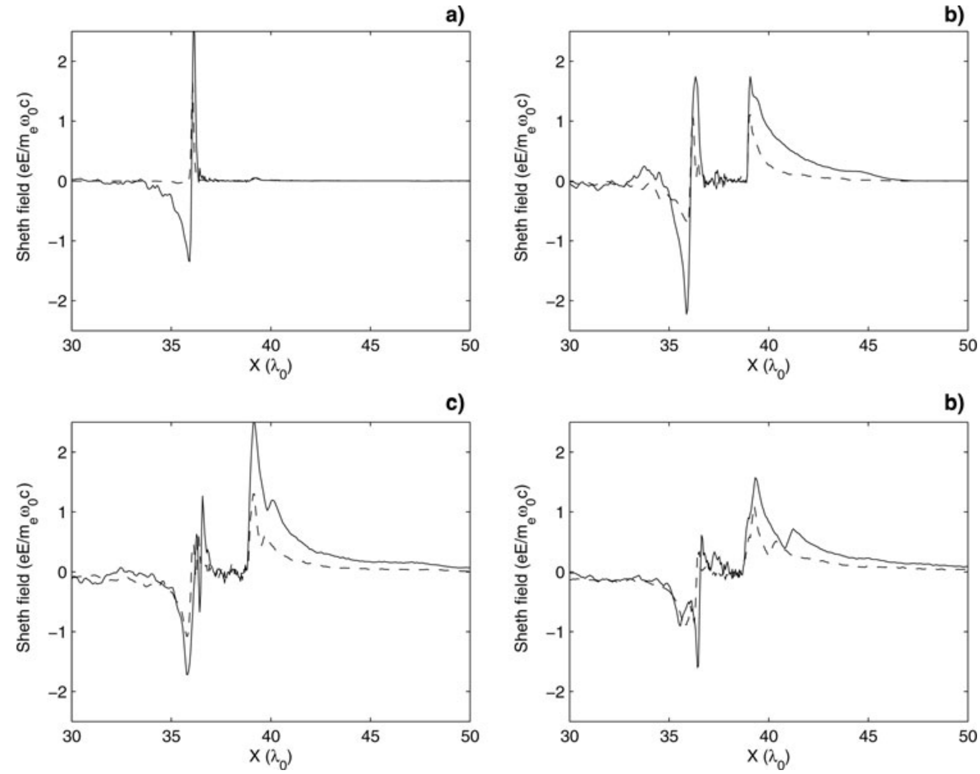

Fig. 2. On-axis distribution of sheath fields for cone target (solid line) and film target (dashed line) at (**a**)$t = 40\tau_0$, (**b**)$50\tau_0$, (**c**)$60\tau_0$, (**d**)$70\tau_0$.

significantly by the focused laser light, and so is the accelerating sheath field.

Figure 3a shows the spatial distribution of laser energy density for cone target. At the cone tip, laser energy density is increased about 6.4 times higher than the incident one. From the scaling law of $J \times B$ mechanism, the temperature of hot electrons should be increased 2.5 times higher. The energy spectra of hot electrons escaping from the targets' rear surface are plotted in Figure 3b. The electron temperature for film target is 1.14 MeV; for cone target it is 3.36 MeV, even higher than the expectation from the scaling law given above. This can be interpreted by the re-acceleration of surface hot electrons by the focused laser light at the cone tip. Therefore, higher hot-electron temperature of the cone target accounts for the higher sheath field at the target's rear surface, which is consistent with the results shown in Figure 2. The energy-transfer ratios from the laser to the hot electrons are 1.9% and 0.7% for the cone target and film target, respectively.

The above results demonstrate that the cone target can obtain higher temperature of hot electrons and the sheath field, which can accelerate protons on the rear surface, than the film target. Figure 4 shows the distribution of both heavy ions and protons in phase space at $t = 70\tau_0$ for cone

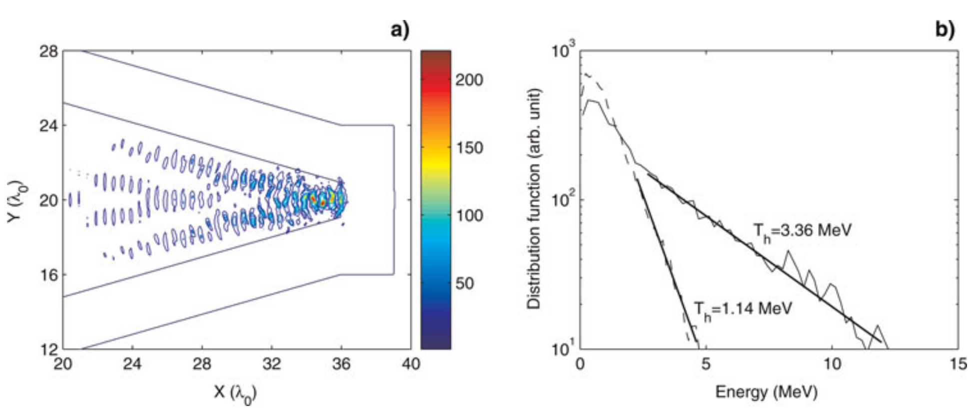

Fig. 3. (Color online) (**a**) spatial distribution of laser energy density at $t = 50\tau_0$ for cone target; (**b**) spectra of electrons escaping from the rear surface of cone target (solid line) and film target (dashed line).

https://doi.org/10.1017/S0263034610000650 Published online by Cambridge University Press

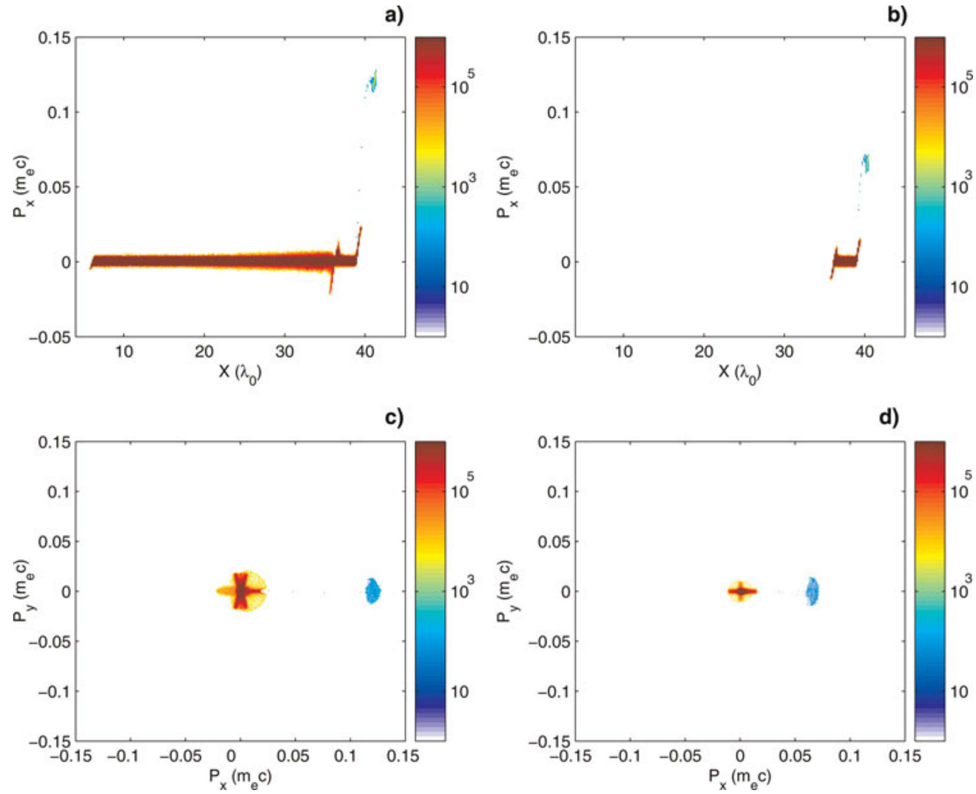

Fig. 4. (Color online) Distribution of ions in phase space p_x *vs* x at $t = 70\tau_0$ for (**a**) cone target and (**b**) film target. Distribution of ions in phase space p_x *vs* p_y at $t = 70\tau_0$ for (**c**) cone target and (**d**) film target.

target and film. At the tip of cone target or front side of film target, a fraction of ions move backward and a fraction of ions move forward, which is consistent with the direction of sheath field shown in Figure 2. Moreover, at the rear surface of the substrate, both heavy background ions and protons are accelerated forward by the sheath field. However, protons are accelerated to higher momentum because of their lighter mass. For cone target, the longitudinal momentums of protons are higher than those of film target according to the increase of sheath field discussed above. Since the angular spread of protons propagating in the vacuum is determined by the ratio of longitudinal momentum and the transverse momentum as $\tan\theta = p_y/p_x$, from the distributions of ions in momentum phase space p_x *vs.* p_y shown in Figures 4c and 4d, we can estimate the angular distribution of proton emission. For film substrate, protons are confined in a cone angle about 26°. For cone substrate, the cone angle is 12°, which means much better collimation than film target.

Figure 5a shows the energy spectra of protons measured at $t = 70\tau_0$, just after the incident laser light interacts with plasma. For the film target (dashed line), the peak proton energy is $E_0 = 2.0$ MeV, and the energy spread is

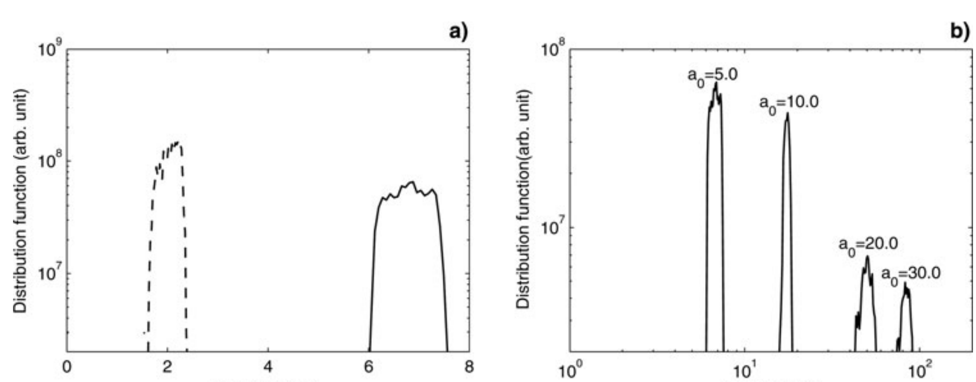

Fig. 5. (**a**) Energy spectra of protons at $t = 70\tau_0$ for cone target (solid line) and film target (dashed line). (**b**) Energy spectra of protons at $t = 70\tau_0$ for $a_0 = 5.0$, 10.0, 20.0 and 30.0.

https://doi.org/10.1017/S0263034610000650 Published online by Cambridge University Press

$\Delta E_{FWHM}/E_0 = 13.1\%$. For the cone target (solid line), the peak proton energy is $E_0 = 6.9$ MeV, 3.5 times higher than that of the film target, and the energy spread is $\Delta E_{FWHM}/E_0 = 16.3\%$. The total energy transported from the laser to protons for the cone target is also about three times increased than the film target, which is consistent with the increase of hot electrons' temperature by cone target. It is confirmed that this cone substrate plus sub-micron proton layer scheme can increase the energy of protons and the coupling from laser to protons by about three times while maintaining the protons' monochromaticity.

Figure 5b shows the energy spectra of protons *vs.* laser intensities. Energy of proton beam is proportional to the normalized laser vector potential, which is consistent with TNSA mechanism and scaling law of J × B mechanism. When $a_0 = 30$, proton beam's energy can be as high as 83 MeV. If three-dimensional effect of the laser focusing from cone target is taken into account, the energy can be high to around 100 MeV. The current petawatt laser facility has intensity over 1.0×10^{20} W/cm^2 and duration about 500 fs, which is longer than that in our simulations and should be advantageous for proton acceleration. If the scheme discussed in this report is carried out under such laser pulse condition, 200 MeV monoenergetic proton beams which are appropriate for cancer therapy may be achieved.

CONCLUSION

In this paper, a target design of a cone-shaped substrate, on the rear surface of which a proton layer is coated, is studied by two-dimensional PIC simulations. It is shown that this scheme can increase the energy of protons and the coupling from laser to protons by about three times while maintaining the monochromaticity of proton beams. This effect is owed to the laser focusing and electron guiding by cone substrate.

ACKNOWLEDGEMENTS

This work was supported by the National Key Laboratory of Laser Fusion. Y. G. thanks the financial support from the Natural Science Foundation of China under grant No. 10975121, and the Science and Technology Foundation of CAEP under grant No. 2006Z0202.

REFERENCES

Birdsall, C.K. & Langdon, A.B. (1991). *Plasma Physics Via Computer Simulation*. New York: McGraw-Hill.

Borghesi, M., Campbell, D.H., Schiavi, A., Willi, O., Mackinnon, A.J., Hicks, D., Patel, P., Gizzi, L.A., Galimberti, M. & Clarke, R.J. (2002). Laser-produced protons and their application as a particle probe. *Laser Part. Beams* **20**, 269–275.

Bulanov, S.V., Esirkepov, T.Z., Khoroshkov, V.S., Kuznetsov, A.V. & Pegoraro, F. (2002). Oncological hadrontherapy with laser ion accelerators. *Phys. Lett. A* **299**, 240–247.

Clark, E.L., Krushelnick, K., Davies, J.R., Zepf, M., Tatarakis, M., Beg, F.N., Machacek, A., Norreys, P.A., Santala, M.I.K., Watts, I. & Dangor, A.E. (2000). Measurements of energetic proton transport through magnetized plasma from intense laser interactions with solids. *Phys. Rev. Lett*. **84**, 670.

Esirkepov, T.Z., Bulanov, S.V., Nishihara, K., Tajima, T., Pegoraro, F., Khoroshkov, V.S., Mima, K., Daido, H., Kato, Y., Kitagawa, Y., Nagai, K. & Sakabe, S. (2002). Proposed double-layer target for the generation of high-quality laser-accelerated ion beams. *Phys. Rev. Lett*. **89**, 175003.

Flippo, K.A., D'humieres, E., Gaillard, S.A., Rassuchine, J., Gautier, D.C., Schollmeier, M., Nurnberg, F., Kline, J.L., Adams, J., Albright, B., Bakeman, M., Harres, K., Johnson, R.P., Korgan, G., Letzring, S., Malekos, S., Renard-Legalloudec, N., Sentoku, Y., Shimada, T., Roth, M., Cowan, T.E., Fernandez, J.C. & Hegelich, B.M. (2008). Increased efficiency of short-pulse laser-generated proton beams from novel flat-top cone targets. *Phys. Plasmas* **15**, 056709–056712.

Kado, M., Daido, H., Fukumi, A., Li, Z., Orimo, S., Hayashi, Y., Nishiuchi, M., Sagisaka, A., Ogura, K., Mori, M., Nakamura, S., Noda, A., Iwashita, Y., Shirai, T., Tongu, H., Takeuchi, T., Yamazaki, A., Itoh, H., Souda, H., Nemoto, K., Oishi, Y., Nayuki, T., Kiriyama, H., Kanazawa, S., Aoyama, M., Akahane, Y., Inoue, N., Tsuji, K., Nakai, Y., Yamamoto, Y., Kotaki, H., Kondo, S., Bulanov, S., Esirkepov, T., Utsumi, T., Nagashima, A., Kimura, T. & Yamakawa, K. (2006). Observation of strongly collimated proton beam from Tantalum targets irradiated with circular polarized laser pulses. *Laser Part. Beams* **24**, 117–123.

Kodama, R., Norreys, P.A., Mima, K., Dangor, A.E., Evans, R.G., Fujita, H., Kitagawa, Y., Krushelnick, K., Miyakoshi, T., Miyanaga, N., Norimatsu, T., Rose, S.J., Shozaki, T., Shigemori, K., Sunahara, A., Tampo, M., Tanaka, K.A., Toyama, Y., Yamanaka, T. & Zepf, M. (2001). Fast heating of ultrahigh-density plasma as a step towards laser fusion ignition. *Nat*. **412**, 798–802.

Li, X.M., Shen, B.F., Zhang, X.M., Jin, Z.Y. & Wang, F.C. (2008). The diagnostics of density distribution for inhomogeneous dense DT plasmas using fast protons. *Laser Part. Beams* **26**, 139–145.

Limpouch, J., Psikal, J., Andreev, A.A., Platonov, K.Y. & Kawata, S. (2008). Enhanced laser ion acceleration from mass-limited targets. *Laser Part. Beams* **26**, 225–234.

Maksimchuk, A., Gu, S., Flippo, K., Umstadter, D. & Bychenkov, V.Y. (2000). Forward ion acceleration in thin films driven by a high-intensity laser. *Phys. Rev. Lett*. **84**, 4108.

Nakamura, T., Mima, K., Sakagami, H., Johzaki, T. & Nagatomo, H. (2008). Generation and confinement of high energy electrons generated by irradiation of ultra-intense short laser pulses onto cone targets. *Laser Part. Beams* **26**, 207–212.

Nakamura, T., Kato, M., Nagatomo, H. & Mima, K. (2004). Surface-magnetic-field and fast-electron current-layer formation by ultraintense laser irradiation. *Phys. Rev. Lett*. **93**, 265002.

Roth, M., Cowan, T.E., Key, M.H., Hatchett, S.P., Brown, C., Fountain, W., Johnson, J., Pennington, D.M., Snavely, R.A., Wilks, S.C., Yasuike, K., Ruhl, H., Pegoraro, F., Bulanov, S.V., Campbell, E.M., Perry, M.D. & Powell, H. (2001). Fast ignition by intense laser-accelerated proton beams. *Phys. Rev. Lett*. **86**, 436.

Schwoerer, H., Pfotenhauer, S., Jackel, O., Amthor, K.U., Liesfeld, B., Ziegler, W., Sauerbrey, R., Ledingham, K.W.D. & Esirkepov, T. (2006). Laser-plasma acceleration of quasi-monoenergetic protons from microstructured targets. *Nat*. **439**, 445–448.

Sentoku, Y., Mima, K., Ruhl, H., Toyama, Y., Kodama, R. & Cowan, T.E. (2004). Laser light and hot electron micro focusing using a conical target. *Phys. Plasmas* **11**, 3083–3087.

Snavely, R.A., Key, M.H., Hatchett, S.P., Cowan, T.E., Roth, M., Phillips, T.W., Stoyer, M.A., Henry, E.A., Sangster, T.C., Singh, M.S., Wilks, S.C., Mackinnon, A., Offenberger, A., Pennington, D.M., Yasuike, K., Langdon, A.B., Lasinski, B.F., Johnson, J., Perry, M.D. & Campbell, E.M. (2000). Intense high-energy proton beams from petawatt-laser irradiation of solids. *Phys. Rev. Lett*. **85**, 2945.

Ter-Avetisyan, S., Schnurer, M., Polster, R., Nickles, P.V. & Sandner, W. (2008). First demonstration of collimation and monochromatisation of a laser accelerated proton burst. *Laser Part. Beams* **26**, 637–642.

Umeda, T., Omura, Y., Tominaga, T. & Matsumoto, H. (2003). A new charge conservation method in electromagnetic particle-in-cell simulations. *Comp. Phys. Commun*. **156**, 73–85.

Wilks, S.C., Kruer, W.L., Tabak, M. & Langdon, A.B. (1992). Absorption of ultra-intense laser pulses. *Phys. Rev. Lett*. **69**, 1383.

Wilks, S.C., Langdon, A.B., Cowan, T.E., Roth, M., Singh, M., Hatchett, S., Key, M.H., Pennington, D., Mackinnon, A. & Snavely, R.A. (2001). Energetic proton generation in ultra-intense laser—solid interactions. *Phys. Plasmas* **8**, 542–549.

Yin, L., Albright, B.J., Hegelich, B.M. & Fernandez, J.C. (2006). GeV laser ion acceleration from ultrathin targets: The laser break-out afterburner. *Laser Part. Beams* **24**, 291–298.